

Design and Validation of Asymmetrically Slotted Ultra Wide Band Antenna for Wireless Communication

Tuhina Oli^{1, *}, Raj Kumar², and Nagendra Kushwaha¹

Abstract—A new compact CPW-fed slot antenna for UWB applications is presented in this paper. The slot in the ground plane is asymmetric which helps in wide band impedance matching. The radiating element is a star-shaped geometry fed by a double stepped co-planar waveguide. Three antennas are designed with this geometry. Out of these three antennas, a compact antenna is proposed. The size of the proposed antenna is $27.2 \times 32.2 \text{ mm}^2$, and it has a measured impedance bandwidth of 8.7 GHz (3–11.7 GHz). The radiation patterns are stable with respect to frequency and of bi-directional shape in E -plane and omnidirectional shape in H -plane. The measured and simulated results are in good agreement.

1. INTRODUCTION

The Federal Communication Commission (FCC) approved frequency band in the range of 3.1 GHz to 10.6 GHz for unlicensed usage in Feb. 2002 [1]. It has motivated both academicians and industrial communities to develop compact antennas for UWB applications. Printed UWB antenna has got maximum attention because the printed antennas have advantage of low profile, light weight and compact geometry [2]. The printed UWB antennas also have advantages such as higher data rate operation with lower power consumption [3]. Numerous methods have been investigated and reported to design UWB antennas, and incorporating a slot in the ground plane is one of the techniques to design these antennas. Ground plane may be incorporated with different slot geometries such as wide or narrow slots [4, 5], square ring slots [6] and U shaped slots [7]. Wider slots provide a greater bandwidth than the narrow ones but have disadvantage of larger size. Other methods employ FSS screens, gap coupled feed [8] and meandered ground planes [9].

In this paper, a CPW-feed slot antenna for UWB applications is presented. The slot in the ground plane is asymmetrically placed, which provides improvement in the impedance matching for the antenna. The patch geometry is star-shaped which is fed by a double stepped feed line.

2. ANTENNA GEOMETRY

Figure 1 shows the structural view of all the antennas. The antennas are printed on one side of a FR4 Epoxy substrate of thickness $h = 1.58 \text{ mm}$, relative permittivity $\epsilon_r = 4.3$ and loss tangent $\tan \delta = 0.019$. Initially a simple symmetric rectangular slot is etched in the ground plane. A double stepped CPW-feed line with widths W_{lf} and W_{uf} and terminated on a star-shaped patch is used to excite the slot. Double stepped CPW feed is used for better impedance matching. The patch is formed by inverting and adding two isosceles triangles with base width denoted by T_b and height T_h , which results in a star-shaped structure as shown in Figure 2. The same patch shape is used in all the antennas but with different sizes. To further increase the bandwidth, the slot is made asymmetric by adding an additional

Received 23 January 2014, Accepted 11 April 2014, Scheduled 15 April 2014

* Corresponding author: Tuhina Oli (tuhinaoli.1989@gmail.com).

¹ DIAT (DU), Girinagar, Pune 411025, India. ² ARDE Pashan, Pune 411021, India.

prototypes are shown in Figure 3, Figure 4 and Figure 5. The measured impedance bandwidth for Antenna 1 is 7.7 GHz (2.6–10.3 GHz), for Antenna 2 7.7 GHz (3–10.7 GHz) and for Antenna 3 8.7 GHz (3–11.7 GHz). The measured and simulated results are in good agreement except for some frequencies. The difference between the measured and simulated results is due to fabrication tolerances and lower quality of SMA connectors. In Figure 5, the measured return loss at around 12 GHz is above -10 dB, which may be due to lower quality of SMA connector used. Figure 6 shows a comparison of the simulated reflection coefficients of all the antennas. It can be seen from Figure 6 that due to variation in the slot shape, antennas have different reflection loss values at the same frequencies. It can also be noticed from Figure 6 that Antenna 1 has smaller bandwidth while Antenna 3 has the largest bandwidth.

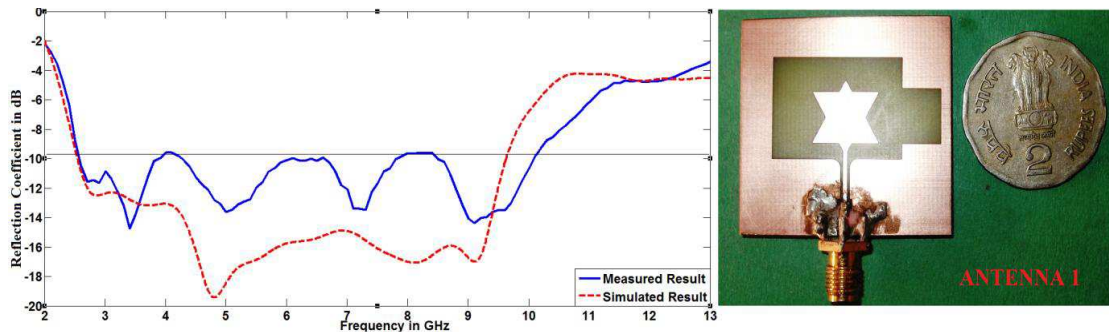


Figure 3. Measured and simulated reflection coefficients of Antenna 1.

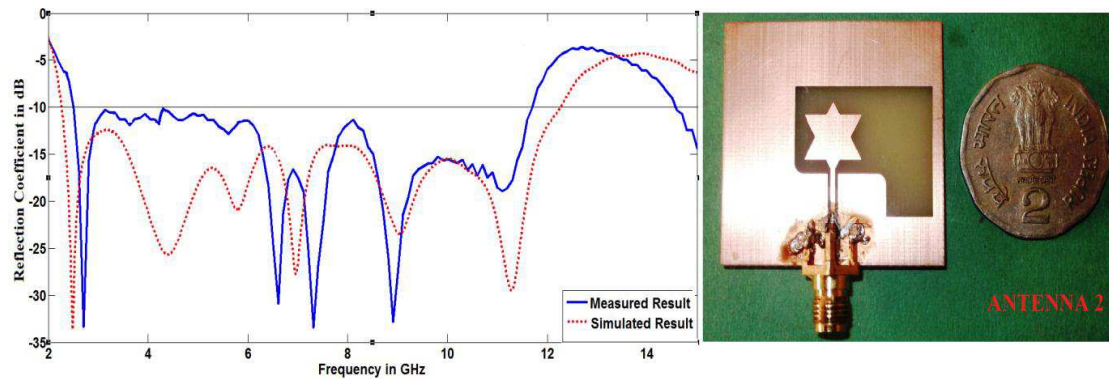


Figure 4. Measured and simulated reflection coefficients of Antenna 2.

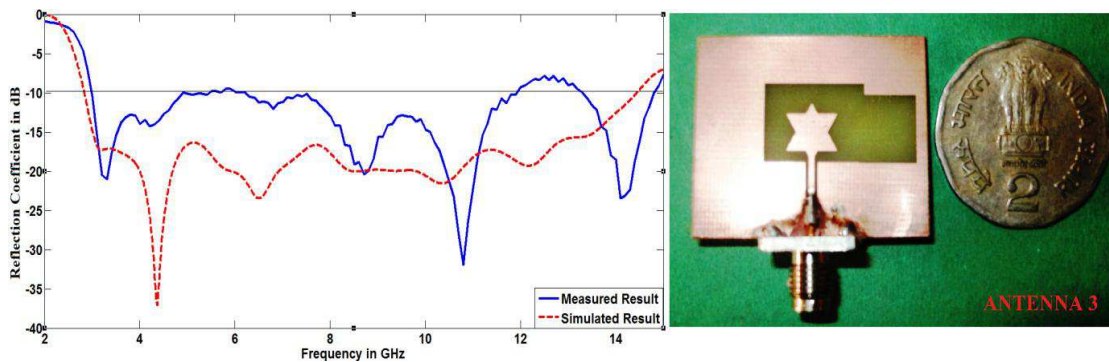


Figure 5. Measured and simulated reflection coefficients of Antenna 3 (proposed antenna).

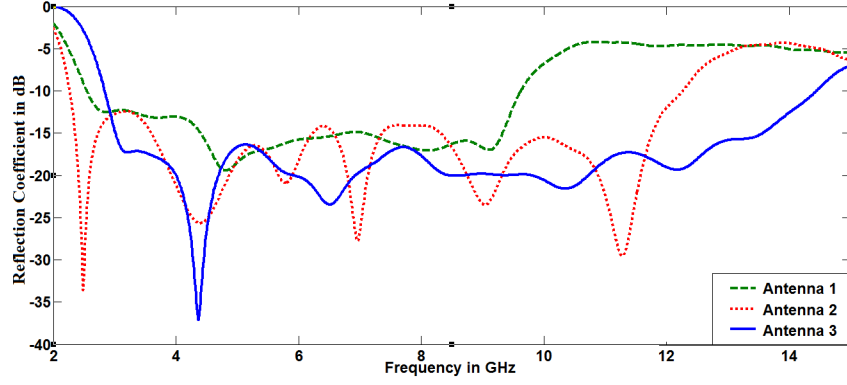


Figure 6. Comparison of simulated reflection coefficients of all three antennas.

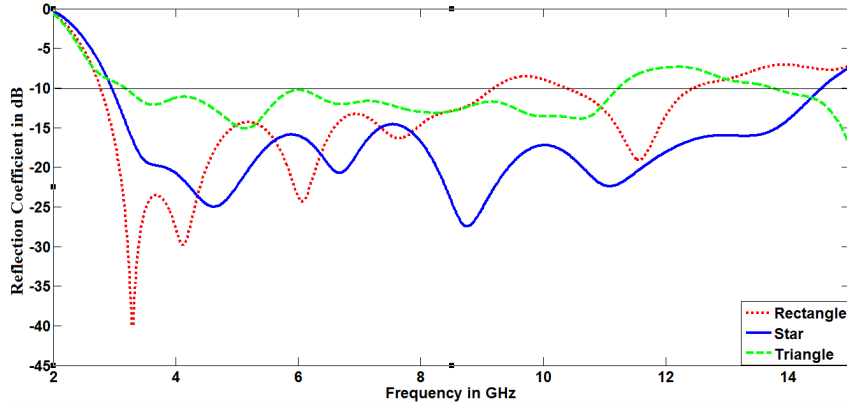


Figure 7. Comparison of return loss of asymmetric slot antenna with different shaped radiating patches.

Figure 7 shows a comparison of the return losses of antenna for different shapes of the patch radiator. The shapes considered are star (proposed), rectangle and triangle. All the shapes have been optimized for maximum bandwidth. It can be seen from the figure that for the asymmetric slot antenna, impedance matching is easier in the case of star-shaped patch than others.

4. THEORETICAL DISCUSSIONS

4.1. Surface Current Distribution

The surface current distributions of the proposed antenna at different resonance frequencies are shown in Figure 8. The red colour shows the maximum current density while the blue shows the minimum current density. The surface current at 3.2 GHz shows two maxima along the slot; therefore, it can be concluded that the resonance at 3.2 GHz is due to the slot in the ground plane. The current distribution at 4.3 GHz shows increased current in the star-shaped patch, so the resonance at 4.3 GHz is due to the star-shaped patch. The current density at 6.5 GHz shows four maxima along the slot; therefore, the resonance at 6.5 GHz is due to second harmonic of the lowest resonance at 3.2 GHz. By considering the current distribution, the first resonance can be approximated as

$$f_1 = \frac{c}{SL\sqrt{\varepsilon_{eff}}} \quad (1)$$

Here f_1 is the lowest resonance frequency in Hz, SL the slot length in meter and equal to 0.065 meter, c the speed of light in m/sec, and ε_{eff} the effective relative permittivity, which can be approximated by $(\varepsilon_r + 1)/2$. The second resonance frequency can be approximated by considering the height of the

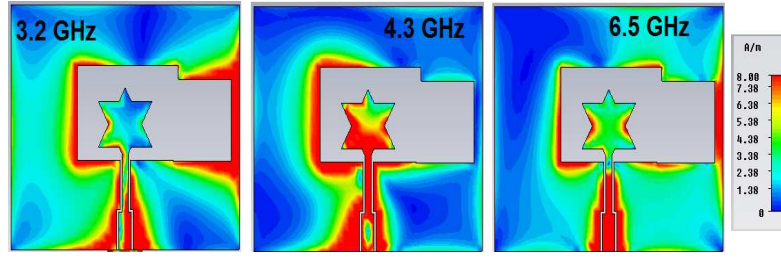


Figure 8. Current distribution for the proposed antenna.

patch to $\lambda/4$ and given by

$$f_2 = \frac{c}{4L\sqrt{\epsilon_{eff}}} \quad (2)$$

Here, L is the height of the star-shaped patch.

4.2. Effect of Asymmetric Slot

For a CPW-fed antenna, the open-end patch adds extra capacitive reactance to the feed line. To neutralize this capacitive effect, an extra inductor needs to be created. If asymmetry is introduced in the ground plane slot, then due to concentration of surface current, an extra inductive reactance is created. This extra inductance neutralizes the capacitive effect of open-ended patch, which results in a better impedance matching. Hence, the introduction of asymmetric slot in the ground plane increases impedance bandwidth. Figure 9 shows a comparison of input port impedance with and without asymmetric slot. From the figure it can be seen that by introduction of asymmetric slot in the ground plane, the real part of input port impedance is shifted towards 50 ohms from a higher value, and imaginary part is shifted towards 0 ohms from either lower or higher values. So, by introduction of asymmetric slot in the ground plane, wider impedance bandwidth can be achieved. Figure 10 shows a comparison of the reflection coefficient of antenna without extended slot, extended asymmetric slot and extended symmetric slot. It can be seen from the figure that the antenna with asymmetric slot has the highest impedance bandwidth due to better impedance matching. The effect of asymmetry is more significant around the middle frequencies (near resonance frequency due to the star-shaped patch). For example, it can be seen from Figure 9 that at 5.3 GHz the value of imaginary part of the input impedance is -25Ω in the case of antenna without extended slot, while 10Ω is for the antenna with extended slot. Hence, the capacitive impedance is changed to inductive impedance, and the real part of input impedance is also changed from 220Ω to 47Ω by introducing asymmetric slot in the ground plane, which helps in improving impedance matching. The same conclusion can be drawn by

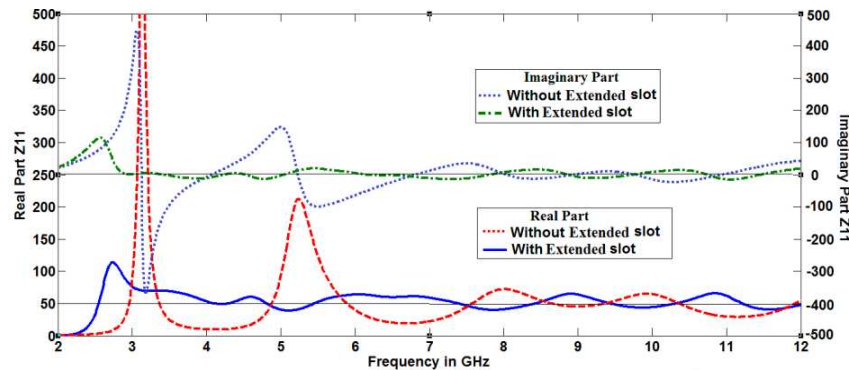


Figure 9. Simulated real and imaginary part of input port impedance of the proposed antenna with and without Slot.

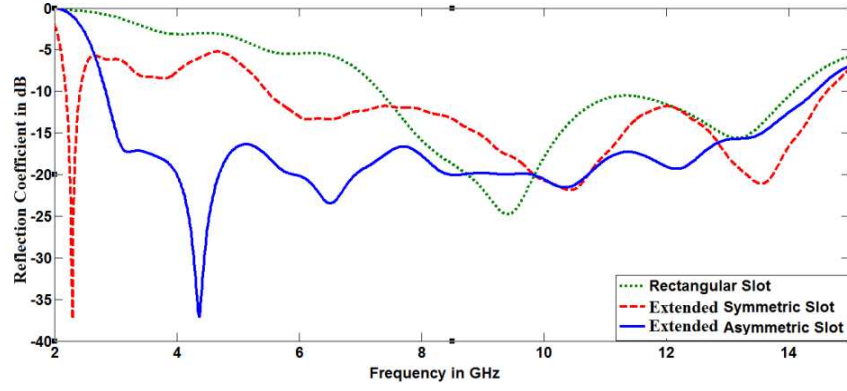


Figure 10. Simulated reflection coefficient comparison for different slot shape of Antenna 3.

observing Figure 10 that at 5.3 GHz the return loss is high in the case of antenna without asymmetric slot compared to the antenna with asymmetric slot.

5. RADIATION PATTERNS AND PEAK GAIN

The radiation patterns of the proposed antenna are measured in an in-house anechoic chamber using antenna measurement system. A double ridged horn antenna is used as reference antenna. Figure 11 shows a comparison of measured and simulated radiation patterns at different frequencies. The simulated radiation patterns in both planes are in good agreement with the measured radiation patterns. The nature of radiation patterns is omnidirectional in *H*-plane and bidirectional in *E*-plane. It is observed that as the frequency increases, the nature of radiation patterns slightly changes which may be because

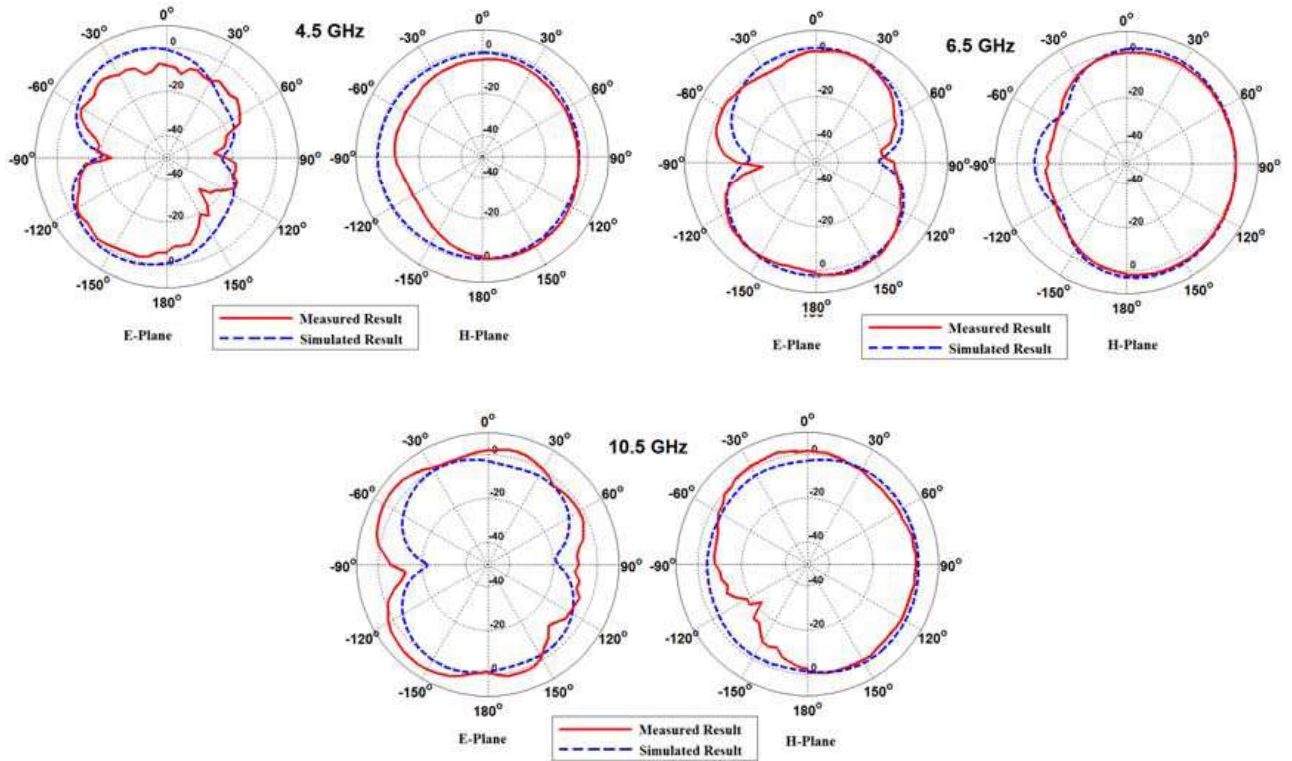


Figure 11. Radiation patterns of the proposed antenna at different frequencies.

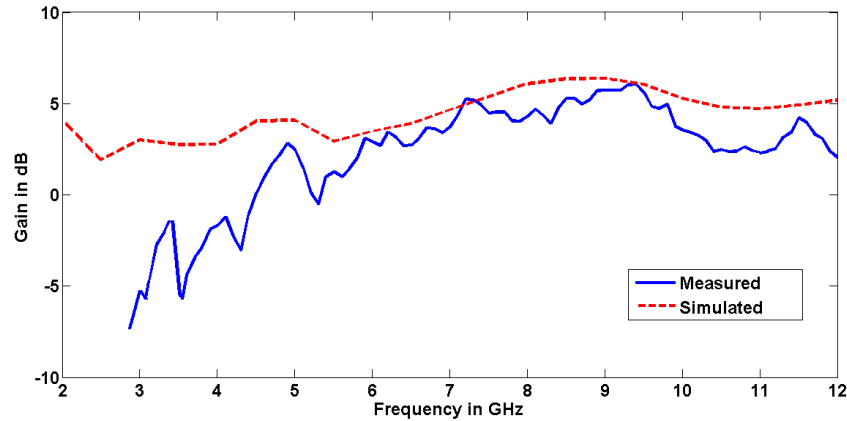


Figure 12. Measured and simulated peak gains of the proposed antenna.

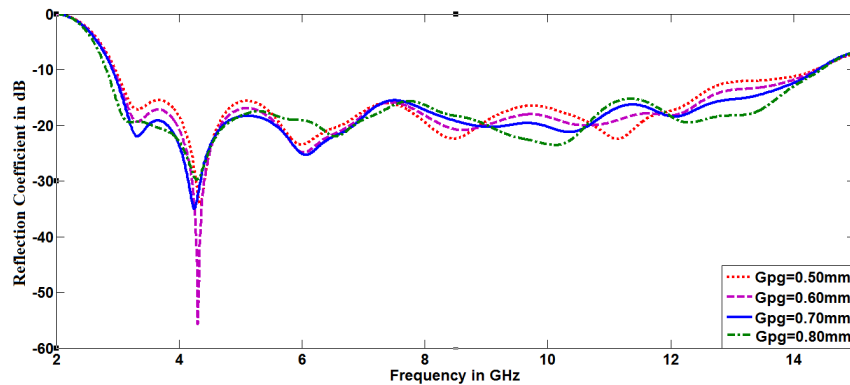


Figure 13. Effect of separation between the patch and the ground plane.

of generation of cross polarization. Figure 12 shows a comparison of measured and simulated peak gains of the proposed antenna. From the figure, it can be seen that the measured gain at low frequencies is less than the simulated gain, because the reference antenna has low gain at low frequencies. The peak gain increases at centre frequencies due to increased impedance matching. Further at higher frequencies, it starts to decrease because of mismatch of impedance and increase in dielectric losses.

6. PARAMETRIC STUDY

6.1. Effect of Separation between Ground Plane and Patch

The coupling between the patch and the ground plane is decided by the separation between the ground plane and the patch. Therefore, the separation is an important parameter which governs the impedance matching, hence the impedance bandwidth. Figure 13 shows the effect of separation between patch and ground on return loss of the proposed antenna. It can be seen from the figure that for higher values of separation, the return loss improves at lower frequencies while deteriorates at higher frequencies. Therefore, there is a need for optimizing separation between the patch and ground. This separation is optimized and found to be 0.7 mm.

6.2. Effect of Asymmetric Slot Dimension

It is noticed that the asymmetric slot dimensions A_2 and B_2 are important parameters which govern the lowest resonance frequency, impedance matching at the middle frequencies, hence the impedance

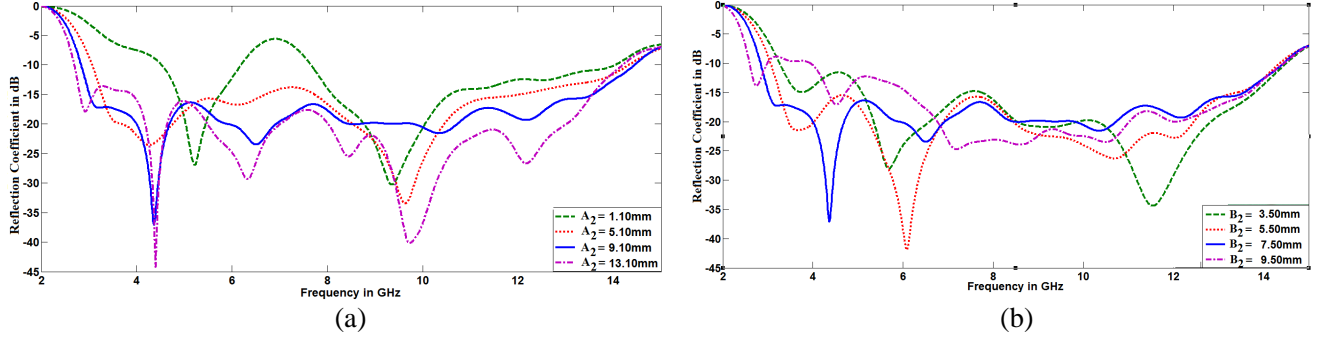


Figure 14. (a) Effect of extended slot length on reflection coefficient of the proposed antenna. (b) Effect of extended slot width on reflection coefficient of the proposed antenna.

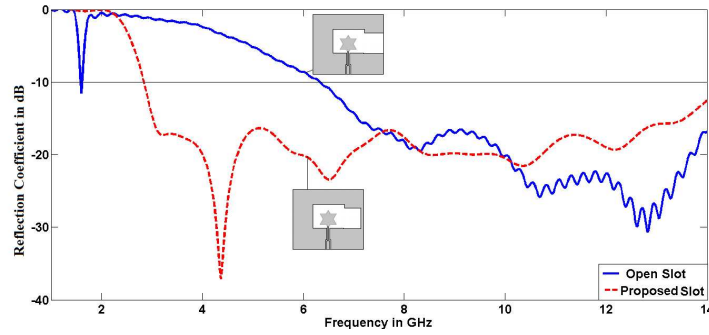


Figure 15. Return loss comparison of proposed antenna with antenna with open ended slot antenna.

bandwidth of the antenna. Figure 14(a) shows the effect of variation of slot length A_2 on return loss of the proposed antenna. It can be seen from the figure that as the length of the asymmetric slot increases, the lower resonance frequency shifts towards lower side due to increase in overall slot length. It is also noticed that as the slot length increases the resonances becomes more dominating. This is due to increased coupling with increase in the asymmetric slot length. Figure 14(b) shows the effect of slot width B_2 on the return loss of the proposed antenna. It can be seen from the figure that with increase in the value of B_2 , the lowest resonance frequency shifts towards the lower side in the same fashion as in the case of variation of asymmetric slot length. After a particular value of B_2 , the return loss at lower frequencies starts deteriorating. So there is a need to optimize the value of B_2 . The value of B_2 is optimized and found to be 7.50 mm.

6.3. Effect of Opening Slot at One End

For the study, the slot is opened at one end. When the slot is opened, the impedance matching deteriorates significantly, and an extra resonance is generated at lower frequency because the open-end slot works as a $\lambda/2$ resonator. Figure 15 shows a comparison of return loss of the proposed antenna with an open-ended slot. It can be seen from the figure that opening the slot at one end, an extra resonance is generated at 1.5 GHz.

7. CONCLUSIONS

Three CPW-feed slot antennas are designed. Out of them, the one with a compact size and wider impedance bandwidth is proposed. The slot in the ground plane is placed asymmetrically which helps in achieving wide band impedance matching. The radiating element is a star-shaped patch fed by a double stepped CPW. The impedance bandwidth is 128% at centre frequency of 7 GHz. It is also noticed that the shape of the slot in the ground plane has a major effect on the impedance bandwidth. The radiation

patterns are measured and found to be bi-directional in E -plane and omnidirectional in H -plane. The proposed antenna can be used for UWB applications such as high-speed data communications and medical imaging.

ACKNOWLEDGMENT

The first author acknowledges the financial support and facilities extended by the Defence Institute of Advanced Technology (Deemed University), Pune, India for carrying out the Research work.

REFERENCES

1. Baskaran, K., C. P. Lee, and K. C. Chandan, "A compact microstrip antenna for ultra wideband applications," *European Journal of Scientific Research*, Vol. 67, No. 1, 45–51, Dec. 2011.
2. Balanis, C. A., *Antenna Theory Analysis and Design*, Wiley-Interscience, 2005.
3. Rafi, G. Z. and L. Shafai, "Wideband V-slotted diamond-shaped microstrip patch antenna," *Electronics Letters*, Vol. 40, No. 19, 1166–1167, 2004.
4. Rama Krishna, R. V. S. and R. Kumar, "Design of ultra wideband trapezoidal shape slot antenna with circular polarization," *AEU — International Journal of Electronics and Communications*, Vol. 67, No. 12, 1038–1047, Dec. 2013.
5. Barbarino, S. and F. Consoli, "UWB circular slot antenna provided with an inverted-L notch filter for the 5 GHz WLAN band," *Progress In Electromagnetics Research*, Vol. 104, 1–13, 2010.
6. Sadat, S., M. Fardis, F. G. Gharakhili, and G. R. Dadashzadeh, "A compact microstrip square-ring slot antenna for UWB applications," *Progress In Electromagnetics Research*, Vol. 67, 173–179, 2007.
7. Lee, K. F., K. M. Luk, K. F. Tong, S. M. Shum, T. Huyn, and R. Q. Lee, "Experimental and simulation studies of the coaxially fed U-slot rectangular patch," *IEEE Proceedings of Microwave Antenna Propagation*, Vol. 144, No. 5, 354–358, Oct. 1997.
8. Hall, P. S., "Probe compensation in thick microstrip patches," *Electronics Letters*, Vol. 23, No. 11, 606–607, 1987.
9. Kuo, J. S. and K. L. Wong, "A compact microstrip antenna with meandering slot in the ground plane," *Microwave and Optical Technology Letters*, Vol. 29, No. 2, 95–97, 2011.